Dephasing of ion beams as the Magnetic Vortex Acceleration regime transitions into a bubble-like field structure

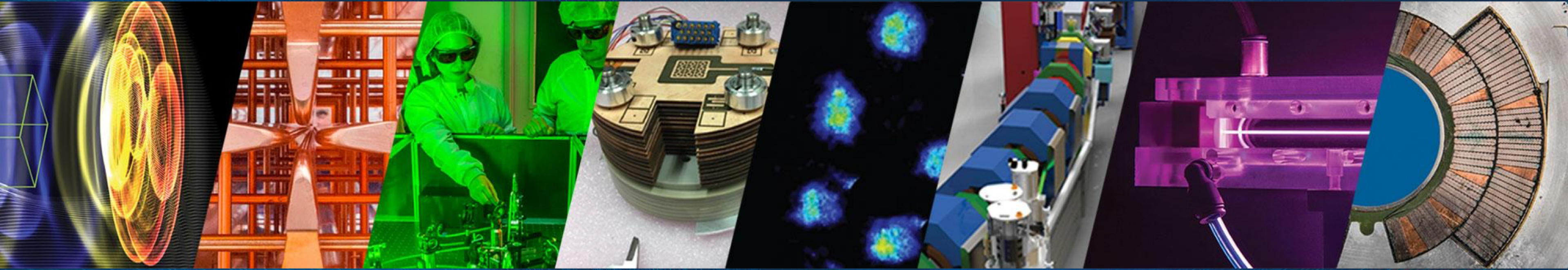

Sahel Hakimi, Stepan S. Bulanov, Axel Huebl, Lieselotte Obst-Huebl, Kei Nakamura, Anthony Gonsalves, Thomas Schenkel, Jeroen van Tilborg, Jean-Luc Vay, Carl B. Schroeder, Eric Esarey, and Cameron R. Geddes

Lawrence Berkeley National Laboratory, Berkeley, California 94720, USA

BERKELEY LAB   ACCELERATOR TECHNOLOGY & APPLIED PHYSICS DIVISION ATAP   LaserNetUS   U.S. DEPARTMENT OF ENERGY | Office of Science

This research is supported by the U.S. Department of Energy (DOE) Fusion Energy Sciences (FES) Postdoctoral Research Program administered by the Oak Ridge Institute for Science and Education (DE-SC0014664). The work is supported by the U.S. DOE Office of Science, Offices of FES and High Energy Physics, LaserNetUS, the Exascale Computing Project (17-SC-20-SC), and used resources at OLCF (DE-AC05-00OR22725) and NERSC (DE-AC02-05CH11231). This research is based upon work supported by the Defense Advanced Research Projects Agency via Northrop Grumman Corporation.

Laser-driven ion sources are of interest for a variety of applications

Discovery Science studies in high energy density science and warm dense matter research

Joseph Cowan & Kirk Flippo, LANL

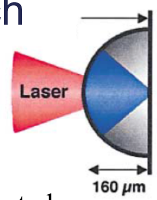

P. Patel et al.
PRL 91.125004 (2003)

Imaging applications

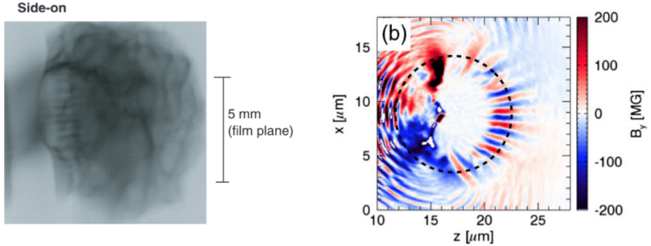

M. Borghesi et al. PPCF 43, A267 (2001)
Göde S et al. PRL 118(19) 194801 (2017)

Material Science

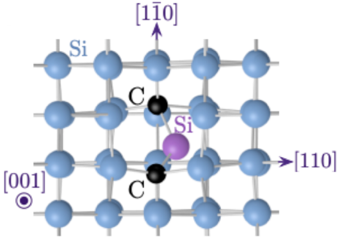

W. Redjem et al. Comm. Materials (2023)

Radiobiological studies

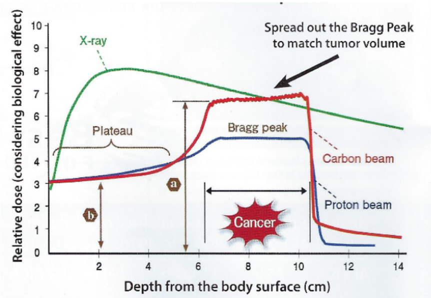

S. V. Bulanov and V. S. Khoroshkov PPR (2002)
H. Tsujii et al. Radiological Sciences, 50(7)4 (2007)

Newly commissioned short focal length beamline at the BELLA PW facility (iP2) to study HEDS

FES funded beamline to investigate ultra-high intensity laser-plasma interactions including advanced ion acceleration mechanisms and applications enabled by laser-driven ions as well as fundamental plasma physics at micron and fs scale

laser parameters	value w/o DPM	anticipated value w DPM
pulse energy [J]	40	24
pulse length [fs]	35	35
energy in FWHM (time)	0.7	0.7
power [PW]	0.8	0.5
wavelength [um]	0.815	0.815
real beam FWHM [um]	2.7	2.7
real beam w0 (gaussian) [um]	2.3	2.3
energy in w0 (space)	0.7	0.7
peak Fluence [J/cm^2]	3.4E+08	2.0E+08
peak Intensity [W/cm^2]	6.8E+21	4.1E+21
av. a0	57	44

K. Nakamura et al. , IEEE JOURNAL OF QUANTUM ELECTRONICS, 53, 4 (2017)
S. Hakimi et al. , Phys Plasmas, 29, 083102 (2022)

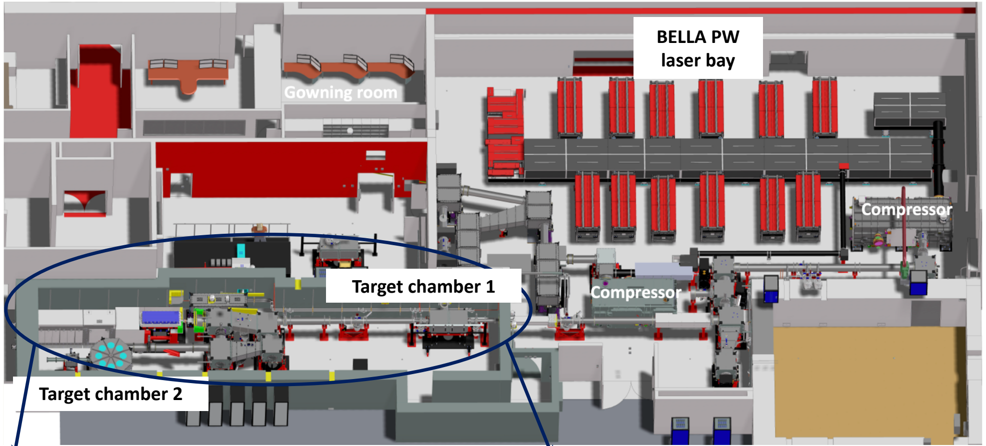

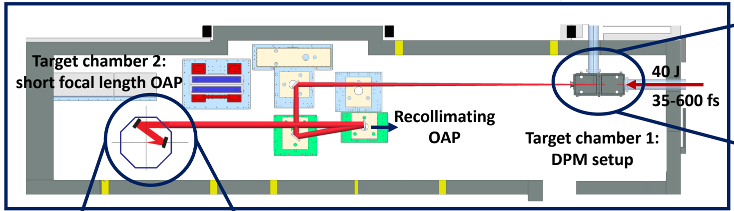

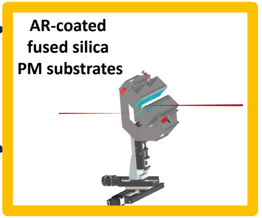

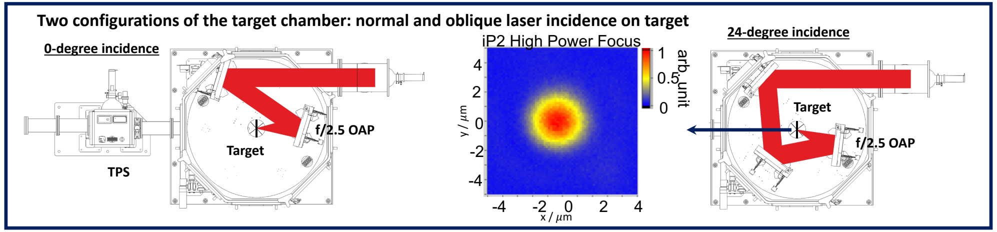

Opportunity to explore ultra-relativistic laser-solid interactions and advanced ion acceleration mechanisms

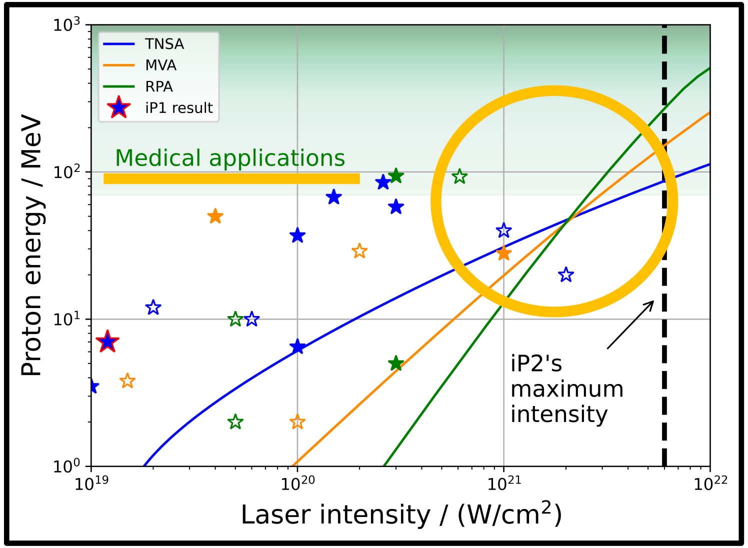

S. Hakimi et al. , Phys Plasmas, 29, 083102 (2022)

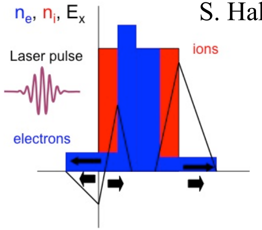

TNSA
Laser: Low intensity
Target: Thick solid density foils
Ion energy: ~100 MeV
Ion energy ~ Laser Power $^{1/2}$

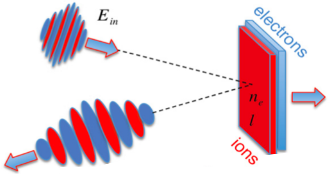

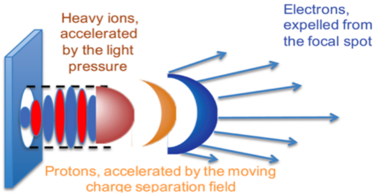

RPA & CE
Laser: High intensity
Target: Thin solid density foils
Ion energy: 100s of MeV
Ion energy ~ Laser Power

MVA
Laser: High intensity
Target: Near Critical Density slab
Ion energy: 100s of MeV to GeV
Collimated ions!
Ion energy ~ Laser Power $^{2/3}$

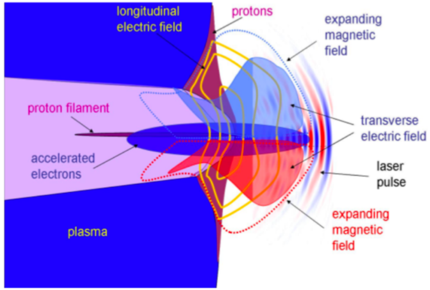

S. S. Bulanov, et al., Physics of Plasmas 23 , 056703 (2016)

The Ion Acceleration Mechanism is Determined by Laser Intensity and Target Surface Density

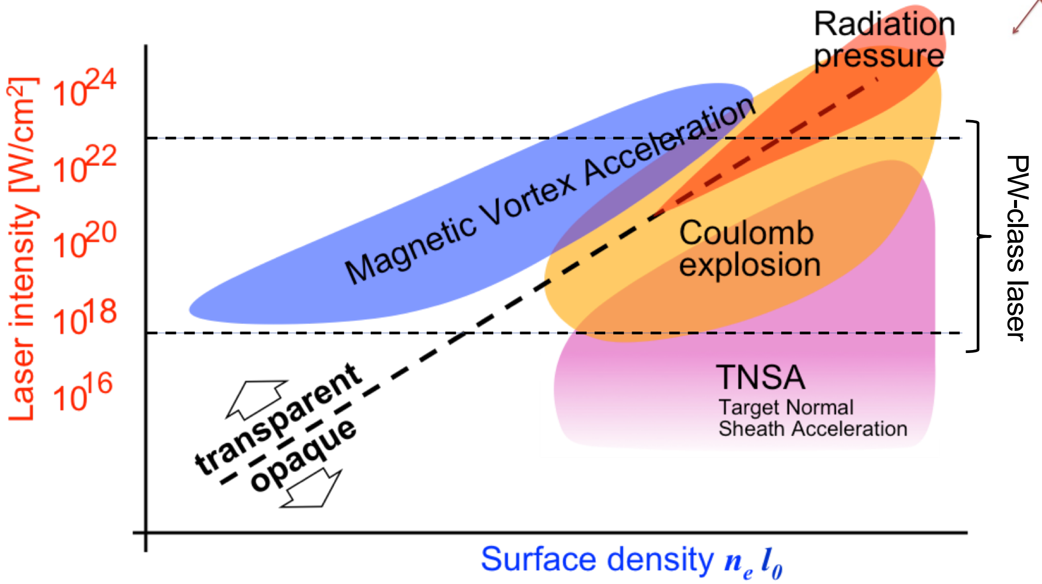

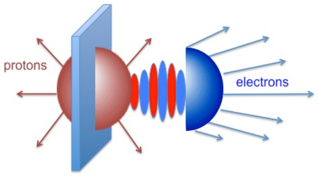

RPA & CE
Laser: High Intensity
Target: Thin solid density foils
Ion Energy: hundreds of MeV
Ion Energy ~ Laser Power

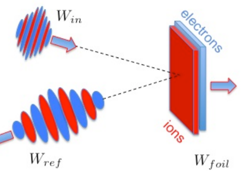

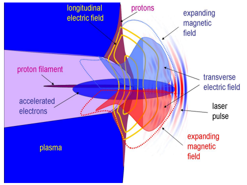

MVA
Laser: High Intensity
Target: Near Critical Density slab
Ion Energy: hundreds of MeV to GeV
Ion Energy ~ Laser Power$^{2/3}$

TNSA
Laser: Low Intensity
Target: Thick solid density foils
Ion Energy: ~100 MeV
Ion Energy ~ Laser Power$^{1/2}$

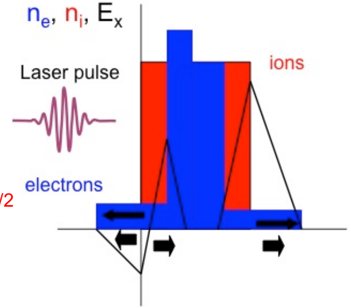

Applications: Radiography, Deflectometry, Cancer Therapy, Injection into conventional accelerators, Fast Ignition, Isochoric heating of matter, Nuclear Physics…

The transparency of the target is one of the most important parameters characterizing laser ion acceleration

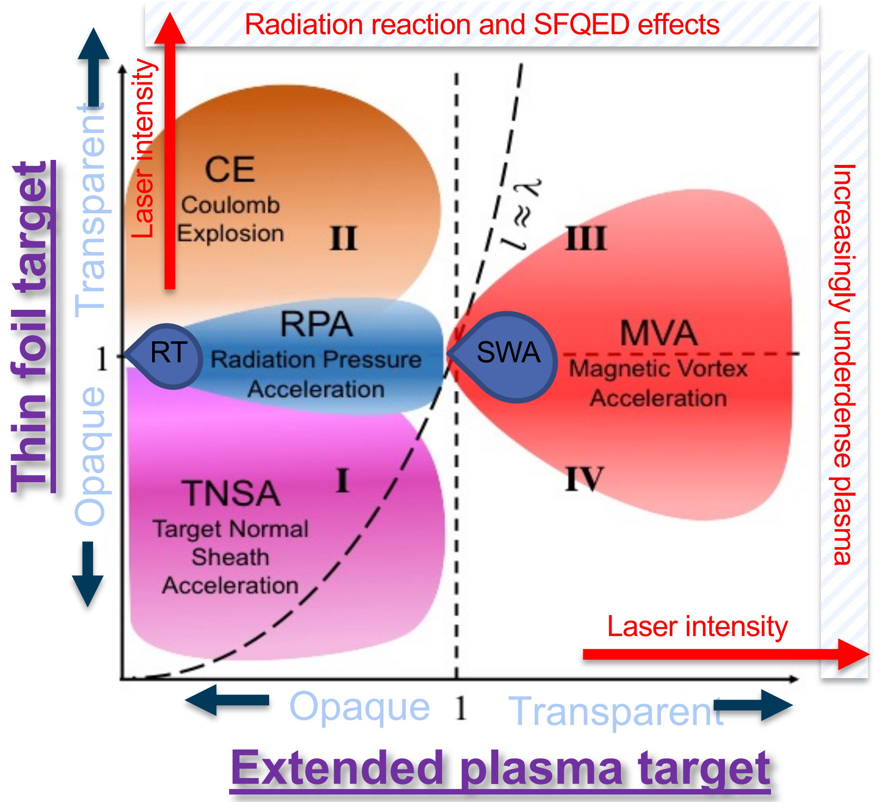

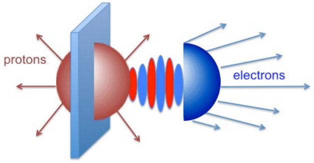

RPA & CE
Laser: High Intensity
Target: Thin solid density foils
Ion Energy: hundreds of MeV
Ion Energy ~ Laser Power

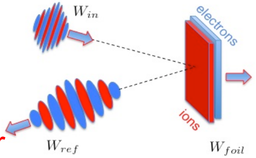

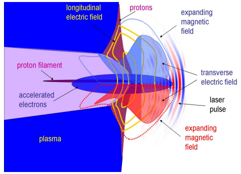

MVA
Laser: High Intensity
Target: Near Critical Density slab
Ion Energy: hundreds of MeV to GeV
Ion Energy ~ Laser Power$^{2/3}$

TNSA
Laser: Low Intensity
Target: Thick solid density foils
Ion Energy: ~100 MeV
Ion Energy ~ Laser Power$^{1/2}$

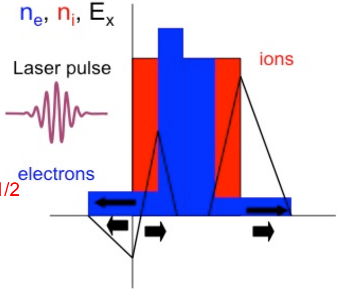

S. S. Bulanov, et al., Physics of Plasmas 23 , 056703 (2016)

Magnetic Vortex Acceleration in Near Critical Density plasma

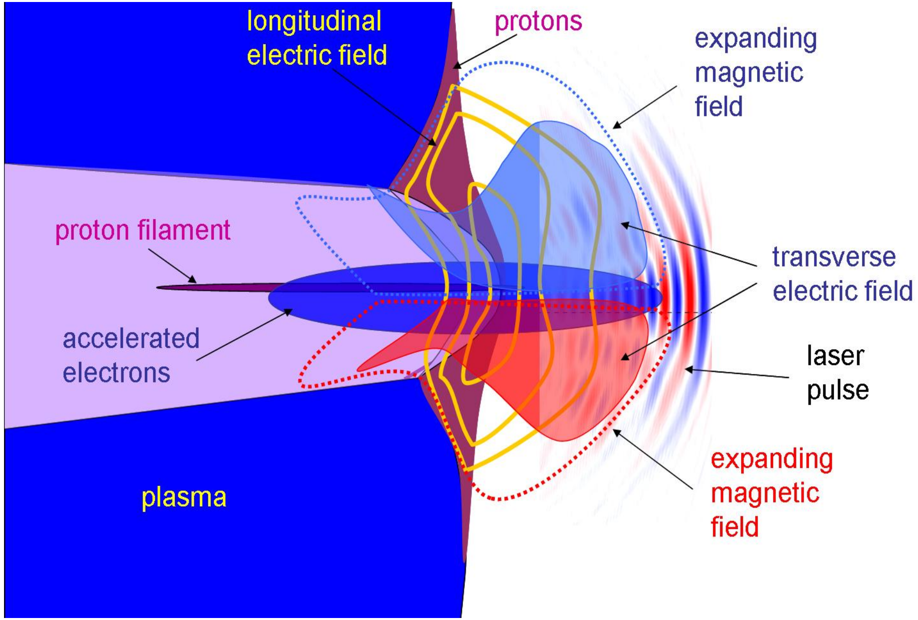

T. Zh. Esirkepov, *et al.*, JETP Lett. 70, 82 (1999).
A. V. Kuznetsov, *et al.*, Plasma Phys. Rep (2001)
L. Willingale, et al., Phys. Rev. Lett (2006)
T. Zh. Esirkepov and S. V. Bulanov, Phys. Rev. Lett. (2006)
A. Yogo, *et al.,* Phys. Rev. E (2008)
Y. Fukuda, *et al*., Phys. Rev. Lett. (2009)
T. Nakamura, *et al*., Phys. Rev. Lett. (2010)
S. S. Bulanov, et al., Phys. Plasmas (2010)
S. S. Bulanov, et al., Phys. Rev. AB (2015)
M. Helle, et al., Phys. Rev. Lett. (2016)
A. Sharma, Sci. Reports (2018)
J. Park, et al., Phys. Plasmas (2019)
S. Hakimi, et al., Phys. Plasmas (2022)
…

Near Critical density Targets:

- Less requirements for laser contrast than in RPA
- Potential high repetition rate operation

Brief overview of the Magnetic Vortex Acceleration mechanism:

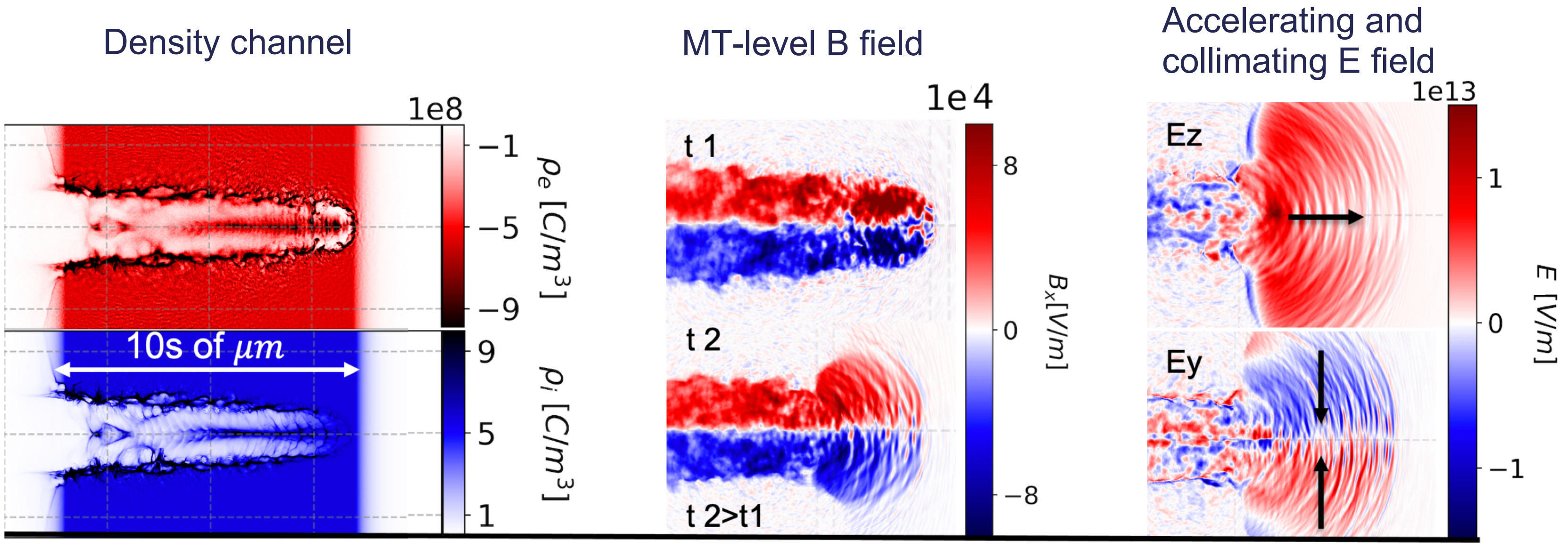

- The laser pulse propagates through a near-critical density target, creating a channel in both electron and ion density
- Accelerated electrons in the channel generate a strong B field (~ 0.1 MegaTesla)
- B field expands as it exits the target and displaces electrons from ions
- This charge separation creates a strong E field that can accelerate and collimate ions from the ion filament

EXASCALE COMPUTING PROJECT

WarpX

Pre-expansion of the NCD target can significantly modify the MVA

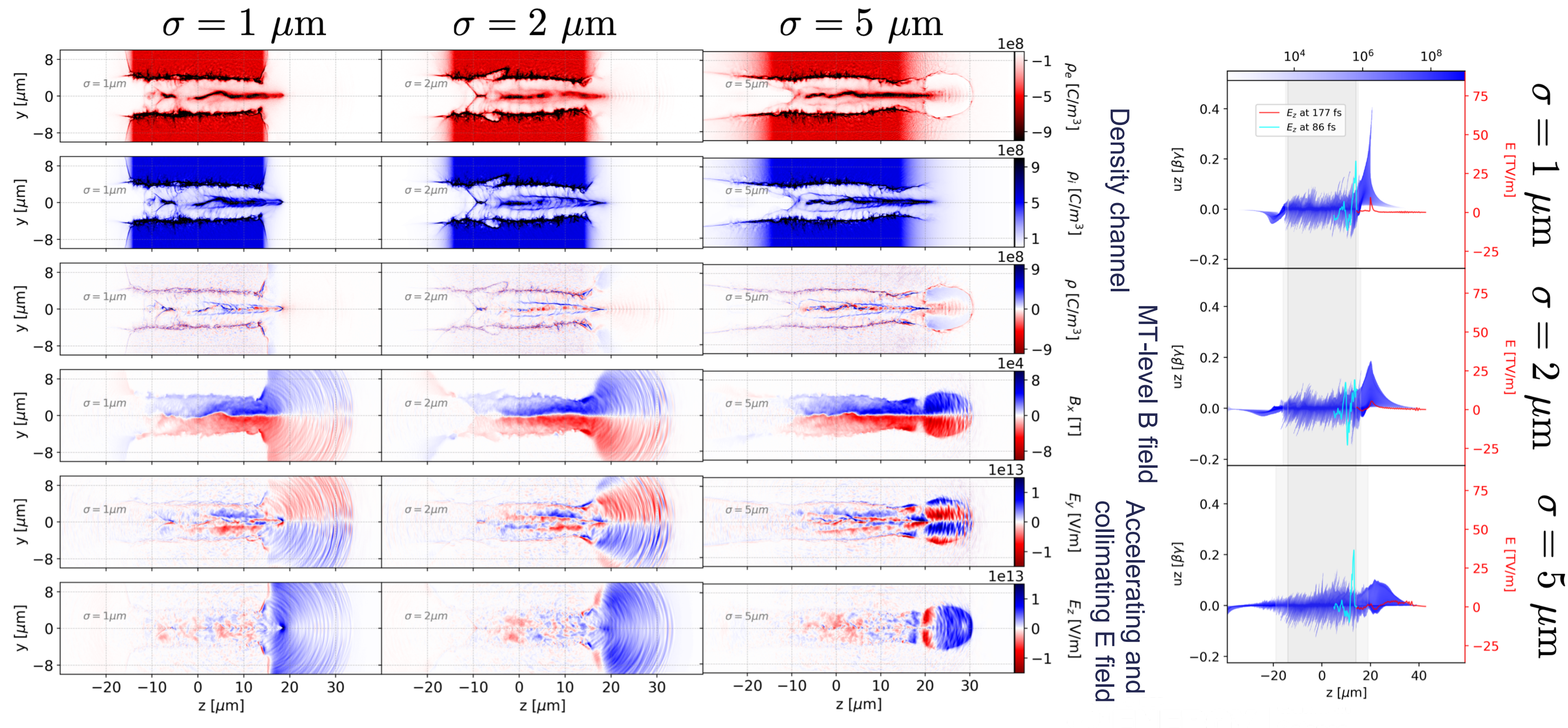

The evolution of accelerated proton beam energy and divergence depend strongly on the pre-plasma scale length

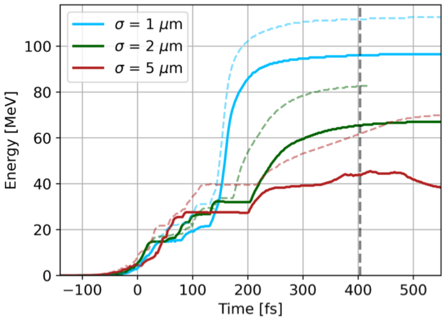

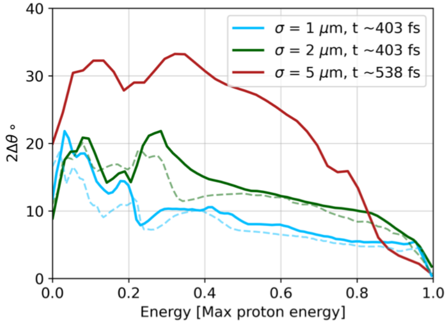

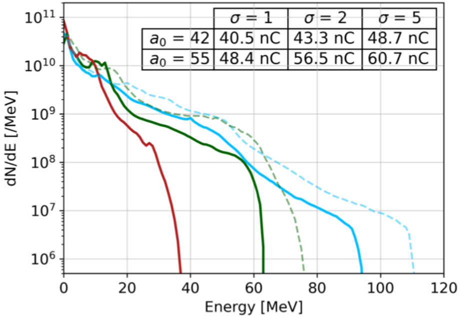

(Left) Maximum proton energy as a function of time for different pre-plasma scale lengths.

(Middle) Proton beam divergence as a function of normalized kinetic energy.

(Right) Proton kinetic energy spectra are shown.

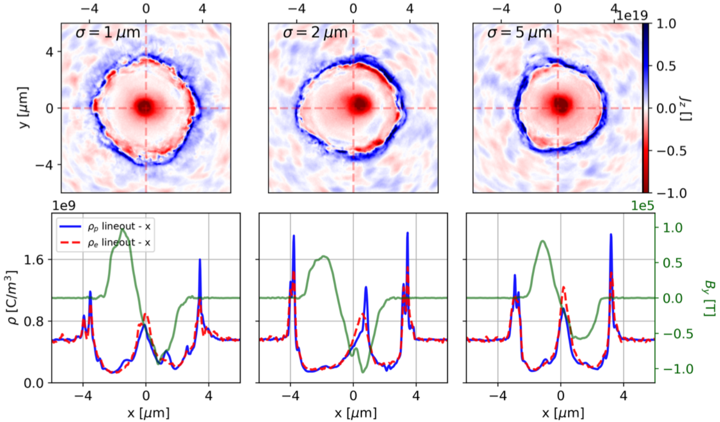

Electric current density, electron and proton density lineouts, and transverse magnetic field lineouts are shown for the three cases of preplasma scale length

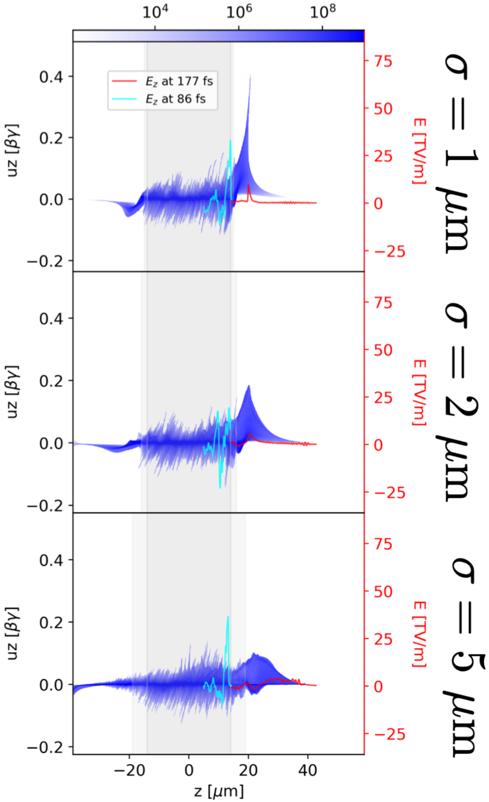

Different pre-plasma scale lengths result in the generation of spatially confined, low divergence proton beams, with low emittance

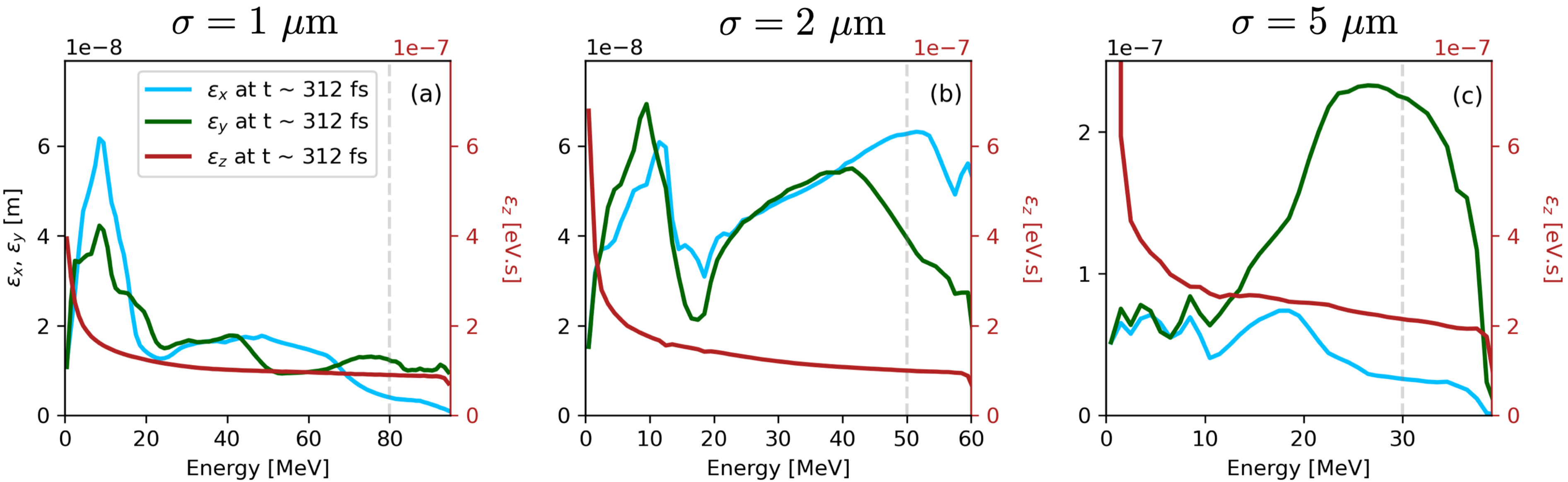

ECP EXASCALE COMPUTING PROJECT

WarpX

Effectiveness of the MVA regime is related to the laser depositing its energy to the fast electrons and exiting the target rear side

- The laser focal spot-size should match the diameter of the self-generated channel

$$R_{ch} = (\lambda/\pi)(n_{cr}/n_e)^{1/3}(2P_{ch}/KP_c)^{1/6} \Rightarrow a_{ch} = (2P_{ch}/KP_c)^{1/3}(n_e/n_{cr})^{1/3}$$

- Laser must propagate and exit through the target without breaking up

$$\frac{L_{ch}}{L_p} = K^{2/3}\left(\frac{2P}{P_c}\right)^{1/3}\left(\frac{n_{cr}}{n_e}\right)^{2/3}$$

$$P_c = 2m_e^2c^5/e^2 = 17\ \mathrm{GW}$$

$$n_{cr} = m_e\omega^2/(4\pi e^2)$$

- With optimized conditions:

$$N_{max} = \frac{\lambda^3 n_{cr}}{4\sqrt{2}\pi^2}\left(\frac{2P_{ch}}{KP_c}\right)^{2/3}\left(\frac{n_e}{n_{cr}}\right)^{1/6}.$$

$$B = 1.1\frac{m_e c}{\lambda}\sqrt{\frac{P_{ch}}{P_c}}$$

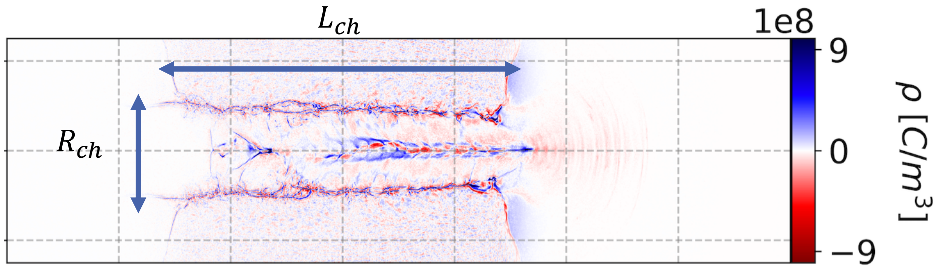

For 1 PW laser pulse and $n_e = 2n_{cr}$ $\Rightarrow$ $B \simeq 0.6$ MT, $N_{max} \simeq 45$ nC

If the laser spot-size is larger than the radius of the self-generated channel it leads to the reduction of MVA effectiveness

- If $w_0 > R_{ch,0}$ the radius of the resulting channel is

$$\frac{\pi R_{ch}}{\lambda} = \left(\frac{n_{cr}}{n_e}\right)^{1/3} \left(\frac{2(R_{ch}/w_0)^2 P}{KP_c}\right)^{1/6} \Rightarrow \frac{R_{ch}}{\lambda} = \left(\frac{n_{cr}\lambda}{\pi^3 n_e w_0}\right)^{1/2} \left(\frac{2P}{KP_c}\right)^{1/4}$$

- The depletion length of the laser in the NCD plasma is reduced

$$\frac{L_{ch}}{L_p} = \frac{K n_{cr}\lambda}{\pi n_e w_0} \left(\frac{2P}{KP_c}\right)^{1/2}$$

- The number of accelerated protons and the amplitude of the magnetic field are reduced as a result:

$$N_{max} = \frac{\lambda^3 n_{cr}}{4\sqrt{2}\pi^4} \frac{2P}{KP_c} \left(\frac{n_{cr}}{n_e}\right)^{1/2} \left(\frac{\lambda}{w_0}\right)^2$$

$$B = 2.5\frac{m_e c}{\lambda} \left(\frac{\lambda}{w_0}\right)^{3/2} \left(\frac{n_{cr}}{\pi^3 n_e}\right)^{1/2} \left(\frac{P}{P_c}\right)^{3/4}$$

For 1 PW laser pulse and $n_e = 2n_{cr}$ ⇒ $N_{max} \simeq 34\ \mathrm{nC}$ and $B \simeq 0.46\ \mathrm{MT}$

Conclusions

- We studied the effects of different pre-plasma scale lengths on the effectiveness of the magnetic vortex acceleration
- We observed that as the scale length was increased the maximum proton energy decreased:
  - For small scale lengths, the accelerating fields are localized near the back of the target and the protons are able to catch up with them and be accelerated
  - For large scale lengths, the accelerating fields instead of being localized continue to move behind the laser pulse and the protons are not able to catch up with them.
- 3D PIC simulations for different pre-plasma scale lengths show the generation of spatially confined, low divergence proton beams, which result into emittance values of $(\epsilon_x, \epsilon_y) \approx (10\ \text{nm},\ 20\ \text{nm})$
- The non-optimal coupling of the laser to the NCD target: $w_0 > \frac{2.75}{(n_e/n_{cr})^{1/3}} P[PW]^{1/6}\ \mu m$ leads to reduced values of the number of accelerated protons and the amplitude of the magnetic field in the channel:

$$N_{max} = \frac{300}{(n_e/n_{cr})^{1/2} w_0[\mu m]^2} P[PW]\ \text{nC}$$

$$B = \frac{2.6}{(n_e/n_{cr})^{1/2} w_0[\mu m]^{3/2}} P[PW]^{3/4}\ \text{MT}$$

Thank you!